CrystEngComm

Accepted Manuscript

ROYAL SOCIETY OF CHEMISTRY

www.rsc.org/crystengcomm

Hollow Hydroxyapatite Spheres Fabrication with Three-Dimensional Hydrogel Template

Zhiyong Li[1], Tao Wen[1], Yunlan Su[1]*, Xiaoxiao Wei[1], Changcheng He[2], Dujin Wang[1]*

1 Beijing National Laboratory for Molecular Sciences, Key Laboratory of Engineering Plastics, Institute of Chemistry, Chinese Academy of Sciences, Beijing 100190, P. R. China

2 College of Chemistry, Beijing Key Laboratory of Energy Conversion and Storage Materials, Beijing Normal University, Beijing 100875, P. R. China.

Abstract: Hydroxyapatite [HAp, $Ca_{10}(PO_4)_6(OH)_2$] crystals were successfully prepared by the combination of electrophoresis approach and ion diffusion method using template of polyacrylamide (PAAm) hydrogel. Flower-like porous hollow HAp spheres were both obtained in the PAAm hydrogel by the two methods. The diameters of the HAp spheres could be controlled in range of 500 nm to 28 μm. The formation of flower-like porous hollow HAp crystals is believed to be the combined result of three-dimensional hydrogel template and electrostatic interaction.

1 Introduction

Hydroxyapatite (HAp, $Ca_{10}(PO_4)_6(OH)_2$), the major inorganic component of biological hard tissues such as bone and tooth, is native to the human body.[1] Due to its biocompatible, bioactive, non-inflammatory, non-toxic and non-immunogenic nature, the synthetic HAp has been widely investigated for applications in drug and gene delivery, tissue engineering and bone repair, and other biomedical areas.[2-9] As we all know, these excellent properties of HAp are determined by their morphology, crystallite size, composition and structure.[10] Hence, several methods, including precipitation hydrolysis, microwave irradiation, sol-gel, hydrothermal, or solvothermal process, have been developed to synthesize HAp with different morphologies and microstructures.[11-21]

Among various kinds of morphologies of HAp microstructures, porous HAp has advantages in the high specific area and the superior surface activity, which offer more potential applications, especially in biomedical applications.[2] The porous structure can influence cell behavior through a promoted interaction between the surfaces of materials and adsorbed proteins. The porous materials can also act as drug carriers for the delivery of pharmaceutical molecules such as ibuprofen, vancomycin.[1] Recently, several groups focus on the synthesis of HAp with flower-like porous morphology by hydrothermal method. Ma has successfully synthesized flower-like HAp by using $CaCl_2$, NaH_2PO_4, and potassium sodium tartrate via a hydrothermal method at 200 °C for 24 hours.[22] Qi *et al.* have reported a novel DNA-templated

hydrothermal strategy for the synthesis of HAp nanosheet-assembled hollow microspheres with a nanoporous structure.[2] Chi's group has synthesized flower-like HAp by a novel bubble-template route. The pore sizes can be well regulated in a wide range from microscale to nanoscale by smartly constructing a kind of CO_2 bubble as a template and precisely adjusting the system pressure.[23] In addition, they also developed flower-like porous carbonated hydroxyapatite (CHAp) microspheres employing different chelating ions by CO_2 bubble template.[24]

As mentioned above, the hydrothermal methods generally require high temperature and pressure, which is not environment-friendly and often not convenient. Hydrogel-mediated crystal growth frequently occurs in nature during the formation of inorganic materials in living organisms, such as bones, teeth, and shells, which is an environment-friendly process and takes place under standard temperature and pressure. Hence, it is meaningful to use hydrogel as the reaction environment for calcium phosphates, thus developing a novel biomimetic synthetic composite biomaterial at low temperatures and obtaining a fundamental understanding of bone mineralization.[25] Several groups have studied the formation of apatite in the hydrogel by ion diffusion method.[25-28] Yokoi et al. have investigated the effects of the ion concentrations, initial pH, diffusion rate of ions and reaction temperature on the crystalline phases and morphology of calcium phosplate in hydrogel containing phosphate ions.[26,27] Although these work obtained the spherical octacalcium phosphate ($Ca_8(HPO_4)_2(PO_4)_4.5H_2O$, OCP), no flower-like porous HAp spheres had been obtained. Meanwhile, the morphologies of calcium phosphate at different sites

are different. Hutchens et al. have fabricated flower-like HAp with a diameter of 1 μm in a bacterial cellulose (BC) hydrogel.[28] However, they neither gave the inner structure information of HAp, nor proposed the formation mechanism. Moreover, the electrophoresis approach was introduced for hydrogels and successfully prepared hydrogel-HAp composite.[29-32] The HAp hollow microspheres were obtained by electrophoresis approach and the "vesicles theory" was proposed to explain the formation mechanism,[31] but little attention was paid to the flower-like morphology of HAp in their work.

Till now, the synthesis of monodisperse HAp spheres with mesoporous structure is a fundamental challenge.[1] In the present study, we successfully obtained the monodisperse flower-like porous hollow HAp spheres in polyacrylamide (PAAm) hydrogel containing Ca^{2+} by both electrophoresis approach and simple ion diffusion method. Different sizes (500 nm - 28 μm) of HAp spheres could be obtained by the two methods. The possible formation mechanism of flower-like porous HAp spheres is proposed on the basis of the "vesicles theory". This work may provide a better fundamental understanding of bone mineralization and contribute to the fabrication of biomimetic bone material.

2 Experimental

2.1 Materials and preparation of the PAAm hydrogel

All chemicals including solvent ethanol were of analytical grade and were used as received. The hydrogel was prepared according to the reference.[33] Pluronic F127 ($EO_{106}PO_{70}EO_{106}$, Pluronic F127, Sigma-Aldrich Co., USA) aqueous solution (10 g

L^{-1}) was irradiated for 8 h with ^{60}Co γ -rays at a dose rate of 10 Gy min^{-1}. The solutions were bubbled with oxygen (50 mL min^{-1}) during the irradiation process. The irradiated PF 127 solution was mixed with an acrylamide (AAm) (ultrapure, BioDev, Japan) aqueous solution (C_M = 7 M), and the volume ratio of the PF 127 solution to the AAm solution was fixed to be 1 : 4. The solutions were transferred to glass molds. Then the systems were deaerated with bubbling nitrogen for 30 min. After being sealed, the hydrogel samples were placed in a water bath at 50 °C for 36 h where they formed hydrogels.

2.2 Precipitation of calcium phosphate crystals

2.2.1 Pretreatment of the hydrogel

The as-prepared PAAm hydrogel samples were swelled in calcium chloride ($CaCl_2$, Alfa Aesar Company) aqueous solutions for 5 days (prepared with 0.4 M Tris-HCl buffer solution at pH = 9, unless otherwise stated) to 95% water contents (unless otherwise stated), and the concentration of $CaCl_2$ in the hydrogels was adjusted to be 0.20 M.

2.2.2 HAp fabrication by the electrophoresis approach

DYCZ-23A electrophoresis apparatus (Beijing Liuyi Instrument Factory, Beijing, China) with a Pt electrode was used for the precipitation of calcium phosphate crystals (Scheme 1a).[34] A $CaCl_2$ aqueous solution (0.2 M) was set in the anode side, and a disodium hydrogen phosphate (Na_2HPO_4, Alfa Aesar Company) aqueous solution (0.12 M) was placed in the cathode side. Different electric currents were applied in the electrophoresis processes.

2.2.3 HAp fabrication by the ion diffusion method

The PAAm hydrogel after pretreatment was placed in a beaker and then adequate Na_2HPO_4 solution was poured into it (Scheme 1b). The beaker was then sealed and held at a pre-established temperature (37 °C). Removal of the disodium hydrogen phosphate solution on the gel occurred after a period of 5 days, and the precipitate together with the PAAm hydrogel was scooped up using a spatula.

2.3 Characterizations

After washing the hydrogel-HAp composites in ultrapure water, the crystalline phases of the sample were characterized using powder X-ray diffraction. The samples were cut into pieces and then dried in the vacuum dryer at 50 ^{o}C until all water was removed. Powder X-ray diffraction patterns were recorded at ambient temperature using a Rigaku D/max-2500 X'Pert instrument, operating with a monochromated Cu Kα radiation source at 40 kV/30 mA. Data were collected with a scanning speed of 4 min^{-1} in the $10° \leq 2\theta \leq 60°$ range.

The samples used for TEM were cut with a microtome at ambient temperature. The inner morphologies of these samples were observed with a JEM-2200FS transmission electron microscope (Tokyo, Japan) at 300 kV.

The samples for SEM were plunged into liquid nitrogen for about 20 min. The frozen samples were subsequently freeze-dried in a FD-1B-50 vacuum freeze dryer (Beijing Boyikang Laboratory Apparatus Co., Ltd. Beijing, China) until all water was removed. The dried samples were cracked to expose their fresh surfaces. After being sputter-coated with Pt for 1 min, the morphologies of these fractured surfaces were

observed with a JEOL JSM-6700 field emission scanning electron microscope with an accelerating voltage of 5 kV. The EDS was performed with a Hitachi S-4300 scanning electron microscope (Tokyo, Japan). The samples for EDS were not sputter-coated with Pt.

3 Results and discussion

To confirm the crystalline phases of calcium phosphate precipitated in the hydrogel, XRD and EDS characterizations were routinely employed to characterize the phase composition. As shown in Fig. 1, the characteristic diffraction peaks were observed at 2θ = 26°, 32°, 39°, 49°, and 53° for all the samples, which were often assigned to HAp. That is to say, all methods could obtain HAp. The broadening of the diffraction peaks implied that the precipitated HAp had a low crystallinity. Fig. 1b shows that HAp prepared from the as-synthesized hydrogels swollen in pure $CaCl_2$ solutions has the lowest crystallinity, which attributes to the lowest pH value in the hydrogel. The XRD results also show that the crystals fabricated by the electrophoresis approach are mixtures of HAp and dicalcium phosphate dihydrate ($CaHPO_4.2H_2O$, DCPD), while the crystals fabricated by the ion diffusion method are mixtures of HAp, DCPD and tricalcium phosphate (TCP). This is also supported by the EDS results (Table 1).

3.1 HAp fabrication by the electrophoresis approach

In previous reports, no attention has been paid to the detailed information on the surface morphologies of HAp fabricated by the electrophoresis approach.[29,31,32] In our previous work,[34] it is discovered that the typical morphology of HAp fabricated by the electrophoresis approach is flower-like porous structure. To investigate the effect of

diffusion rate on the morphology of HAp, different currents were selected when the hydrogel were swelled in $CaCl_2$ solution (Tris-HCl, pH = 9.0). As seen in Fig. 2, the HAp porous spheres were composed of thin flakes with high aspect ratios. The sizes of HAp spheres obtained at 5 mA and 40 mA are almost the same (ca. 2 μm in diameter). But when the current is elevated to 80 mA, the diameter of the HAp spheres is only as small as 500 nm. Obviously, the current can seriously affect the size of the mineralization products.

To obtain more information about the microstructure of flower-like porous HAp spheres, we characterized the composite samples with TEM (see in Figs. 3a-3c). HAp spheres fabricated at 5 and 40 mA show an obvious hollow structure (marked with a red circle), but not for the one at 80 mA. The hollow structure has also been supported by SEM (Figs. 3d and 3e). In addition, the significant difference between the sizes of the HAp spheres fabricated with 5 and 80 mA is consistent with SEM results. The "vesicles theory" has been proposed to explain the formation mechanism of the hollow HAp spheres.[31] In Fig. 3a, there is an obvious black circle (indicated by a white arrow) which should be induced by the vesicles, and we believe that it is a direct experiment evidence of the "vesicle theory"[31]. In fact, the red circle in Fig. 3a is the completion location of HAp spheres nucleated from the black circle of vesicles. Liu et al. indicated that the size of the vesicles formed by phase separation was affected by the concentration of PAAm polymer.[31] Furthermore, our TEM results show that the current also affects the size of the vesicles. The bigger the current is, the smaller the vesicles are (Figs. 3a and 3c). Meanwhile, the higher current leads to a

faster ion diffusion rate and higher ion concentration, which could provide more nucleation sites for the formation of HAp inside the vesicles. Hence, the HAp nanofibers precipitate much denser inside the vesicles and no obvious hollow structures were observed in the HAp spheres fabricated with 80 mA. In addition, the HAp grows on both sides of the black circle as the ions diffuse to the nucleation sites, owing to driving force imposed by the appli ed voltage. The needle-shaped HAp nanofibers outside of the circle disperse more orderly and much denser than those inside of the circle, because there are more nucleation sites and ions outside of the circle in comparison with the small domain inside of the circle, which can be assured by the TEM results (Fig. 3c).

3.2 HAp fabrication by simple ion diffusion method

In order to investigate the effect of diffusion rate on the HAp morphology and learn the details of HAp's crystallization process in a hydrogel system, we also precipitated HAp by ion diffusion method, which offers a slower ion diffusion rate than electrophoresis approach does. The HAp crystals fabricated by ion diffusion method are also flower-like porous hollow spheres with 2 μm in diameter (Fig. 4 and Fig. S1). It is obvious that they are similar to HAp fabricated by electrophoresis approach with 5 mA (Figs. 2a and 2d). The possible reason is the similar ion diffusion rates in both cases. Furthermore, to eliminate the effect of Tris-HCl buffer solution on the growth of HAp, we fabricated HAp in a hydrogel swelled in pure $CaCl_2$ solution by ion diffusion method. As shown in Figs. 5a and 5b, the HAp particles are also flower-like porous spheres with a diameter of 28 μm. The larger sizes of HAp spheres result from

the absence of the Tris-HCl. Compared to the hydrogels swelled in Tris-HCl (pH = 9.0) $CaCl_2$ solution, the hydrogels swelled in pure $CaCl_2$ solutions have low pH value (~ 7.0), which results in a slower diffusion rate and thus the increasing difficulty for the form of HAp in the interior of hydrogel. And the diffusion rate of ions may also affect the sizes of vesicles. The slower the diffusion rate is, the bigger the vesicles are. Therefore the size of HAp spheres is bigger than those fabricated in the hydrogel swelled in Tris-HCl $CaCl_2$ solution.

In addition, the spheres show a solid core with 5 μm in diameters (domains marked by a red circle in Fig. 5c), which is obviously different from the surrounding. The HAp particles obtained at about 36 hours still exhibit hollow structures (Fig. S2), which should develops from the vesicles. With time increasing, they grow denser and gradually form a solid core. The cross section of the HAp spheres shows the radiation pattern from the center (marked with a white arrow in Fig. 5d), indicating that the diffusion of PO_4^{3-}, HPO_4^{2-}, OH^- into the central part of the spherical domain promote the depletion of calcium ions and the simultaneous crystal growth of HAp.

Time-dependent growth experiment has been carried out to learn the details of HAp crystallization process in a hydrogel system and observe the structure of HAp at different growth time. At the early stage, the typical smooth spheres with uniform size of ~ 700 nm are observed (shown in Fig. 6a and Fig. S3). The sizes of the smooth spheres (~700 nm) based on the vesicles could match the sizes of the central hole of hollow spheres shown by SEM images (Fig. S1) and TEM images (Fig. 3b, marked by a red circle). In succession, the initial smooth crystals grow bigger and the

elementary flower-like porous microspheres are formed (Fig. 6b). As the reaction time goes on, the elementary flower-like porous microspheres grow much bigger and finally reach a diameter of ~ 2 μm (Figs. 6c and 6d).

3.3 The possible formation mechanism of HAp

On the basis of the experimental results above, a possible growth mechanism of the flower-like porous HAp structures is illustrated by cartoon in Scheme 2. On the whole, the hydrogels provide a three-dimensional template for the growth of HAp, which makes it possible that the ions diffuse into the hydrogel slowly and are well-organized. Previous studies have claimed that functional groups such as hydroxyl and carboxyl groups favour the nucleation of calcium phosphate. As shown in Scheme 2a and 2d, the carbonyl groups of the PAAm provide a binding place for the Ca^{2+} ions. Then, phase separation (a salt-out effect) promotes the formation of spherical aqueous domains (vesicles) with a relatively large ionic content inside the organic matrix.[31] When the phosphate ions diffuse into the gel and the ion pairs (Ca^{2+} and PO_4^{3-}) are supersaturated, the vesicles serve as the nucleation centers and then a 3D crystal nucleus forms. As the reaction time goes on, ions diffuse to the reaction system and the crystals will further grow on both sides (outside and inside) of the vesicle (shown in Scheme 2b). Owing to the high surface energy of the nanocrystals and the electrostatic interaction between PAAm molecules and HAp sheets, the newly formed HAp sheets organize in a certain orientation to reduce their surface energy.[2] In this way, HAp nanosheets self-assemble to form flower-like porous spheres gradually (Scheme 2b, 2c). In addition, the different environments between the inner and outer

of the vesicles lead to different crystal morphologies.

4 Conclusions

In summary, we documented a sample system only containing PAAm hydrogel for a better mimicking of calcium phosphate biomineralization process in nature. The flower-like porous hollow HAp spheres were obtained by diffusion of phosphate ions into PAAm hydrogels containing calcium ions by both the electrophoresis approach and the ion diffusion method, and the hydrogels were thus transformed into calcified materials. By interrupting the reaction at different time intervals, the crystallization process was successfully traced and the crystal formation mechanism was proposed. The flower-like porous hollow HAp spheres might be a combination result of hydrogel template and electrostatic interaction.

Acknowledgements

The financial support from the Strategic Priority Research Program of the Chinese Academy of Sciences (XDA01020304) and International Science & Technology Cooperation Program of China (2013DFG52300) is gratefully acknowledged.

References

1 Y.P. Guo, Y.B. Yao, Y.J. Guo and C.Q. Ning, *Microporous Mesoporous Mater.*, 2012, 155, 245-251.
2 C. Qi, Y.J. Zhu, B.Q. Lu, X.Y. Zhao, J. Zhao and F. Chen, *J. Mater. Chem.*, 2012, 22, 22642-22650.
3 A.T. Neffe, A. Loebus, A. Zaupa, C. Stoetzel, F.A. Muller and A. Lendlein, *Acta Biomater.*, 2011, 7, 1693-1701.
4 G. Hulsart-Billstrom, Q. Hu, K. Bergman, K.B. Jonsson, J. Aberg, R. Tang, S. Larsson and J. Hilborn, *Acta Biomater.*, 2011, 7, 3042-3049.
5 L.C. Wu, J. Yang and J. Kopecek, *Biomaterials*, 2011, 32, 5341-5353.
6 W. Cui, X. Li, C. Xie, H. Zhuang, S. Zhou and J. Weng, *Biomaterials* , 2010, 31, 4620-4629.
7 A.K. Gaharwar, S.A. Dammu, J.M. Canter, C.J. Wu and G. Schmidt, *Biomacromolecules*, 2011, 12, 1641-1650.
8 Y. Xu, D. Zhang, Z.L. Wang, Z.T. Gao, P.B. Zhang and X.S. Chen, *Chinese J. Polym. Sci.*, 2010, 29, 215-224.

9 K. Zhang, M. Zhao, L. Cai, Z.K. Wang, Y.F. Sun and Q.L. Hu, *Chinese J. Polym. Sci.*, 2010, 28, 555-561.
10 S.D. Jiang, Q.Z. Yao, G.T. Zhou and S.Q. Fu, *J. Phys. Chem. C*, 2012, 116, 4484-4492.
11 K. Kandori, N. Horigami, A. Yasukawa and T. Ishikawa, *J. Am. Ceram. Soc.*,1997, 80, 1157-1164.
12 J. Liu, K. Li, H. Wang, M. Zhu, H. Xu and H. Yan, *Nanotechnology*, 2005, 16, 82-87.
13 A. Bigi, E. Boanini and K. Rubini, *J. Solid State Chem.*, 2004, 177, 3092-3098.
14 C. Zhang, J. Yang, Z. Quan, P. Yang, C. Li, Z. Hou and J. Lin, *Cryst. Growth Des.*, 2009, 9, 2725-2733.
15 M.G. Ma and J.F. Zhu, *European J. Inorg. Chem.*, 2009, 36, 5522-5526.
16 W. He, J. Tao, H. Pan, X. Xu and R. Tang, *Chem. Lett*., 2010, 39, 674-675.
17 M.G. Ma, Y.J. Zhu and J. Chang, *J. Phys. Chem. B*, 2006, 110, 14226-14230.
18 J.J. Diegmueller, X. Cheng and O. Akkus, *Cryst. Growth Des.*, 2009, 9, 5220-5226.
19 D. Hagmeyer, K. Ganesan, J. Ruesing, D. Schunk, C. Mayer, A. Dey, N.A. Sommerdijk and M. Epple, *J. Mater. Chem.*, 2011, 21, 9219-9223.
20 F. Wang, Y. Guo, H. Wang, L. Yang, K. Wang, X. Ma, W. Yao and H. Zhang, *CrystEngComm*, 2011, 13, 5634-5637.
21 H. Zhou and J. Lee, *Acta biomater.*, 2011, 7, 2769-2781.
22 M.G. Ma, Int. j. *Nanomed.*, 2012, 7, 1781-1791.
23 X. Cheng, Q. He, J. Li, Z. Huang and R.A. Chi, *Cryst. Growth Des.*, 2009, 9, 2770-2775.
24 X. Cheng, Z. Huang, J. Li, Y. Liu, C. Chen, R.A. Chi and Y. Hu, *Cryst. Growth Des.*, 2010, 10, 1180-1188.
25 T. Yokoi, M. Kawashita, G. Kawachi, K. Kikuta and C. Ohtsuki, *J. Mater. Res.*, 2011, 24, 2154-2160.
26 T. Yokoi, M. Kawashita, K. Kikuta and C. Ohtsuki, *Mat. Sci. Eng. C*, 2010, 30, 154-159.
27 T. Yokoi, M. Kawashita, K. Kikuta and C. Ohtsuki, *J. Cryst. Growth*, 2010, 312, 2376-2382.
28 S.A. Hutchens, R.S. Benson, B.R. Evans, H.M. O'Neill and C.J. Rawn, *Biomaterials*, 2006, 27, 4661-4670.
29 J. Watanabe and M. Akashi, *Biomacromolecules*, 2006, 7, 3008-3011.
30 J. Watanabe and M. Akashi, *Cryst. Growth Des.*, 2008, 8, 478-482.
31 G. Liu, D. Zhao, A.P. Tomsia, A.M. Minor, X. Song and E. Saiz, *J. Am. Chem. Soc.*, 2009, 131, 9937-9939.
32 M. Kamitakahara, K. Kimura and K. Ioku, *Colloid Surface B*, 2012, 97, 236-239.
33 C.C. He, K.X. Jiao, X. Zhang, M. Xiang, Z.Y. Li and H.L. Wang, *Soft Matter*, 2011, 7, 2943-2952.
34 Z.Y. Li, Y.L. Su, B.Q. Xie, H.L. Wang, T. Wen, C.C. He, H. Shen, D.C. Wu and D.J. Wang, *J. Mater. Chem. B*, 2013, 1,1755-1764.

Table 1

The Ca/P ratio of the particles characterized by EDS.

samples	**electrophoresis approach**		**ion diffusion method** (in pure $CaCl_2$ solutions)		**ion diffusion method** (in Tris-HCl $CaCl_2$ solutions)	
Element	Wt%	At%	Wt%	At%	Wt%	At%
PK	31.52	32.81	27.53	26.25	33.04	33.26
CaK	58.17	46.79	60.70	44.62	54.19	42.16
Ca/P		1.43		1.70		1.27

Figure Captions

Scheme 1 Schematic illustration of HAp precipitation in the hydrogels containing Ca^{2+} (a) electrophoresis approach; (b) ion diffusion method.

Fig. 1 XRD patterns of the calcium phosphate. (a) Calcium phosphate prepared from the as-synthesized hydrogels swollen in Tris-HCl $CaCl_2$ solutions with pH = 9.0 by electrophoresis approach, (b) Calcium phosphate prepared from the as-synthesized hydrogels swollen in pure $CaCl_2$ solutions using ion diffusion method, (c) Calcium phosphate prepared from the as-synthesized hydrogels swollen in Tris-HCl $CaCl_2$ solutions with pH = 9.0 using ion diffusion method.

Fig. 2 SEM micrographs of HAp spheres templated with the hydrogels using different currents (a, d) 5 mA (b, e) 40 mA, (c, f) 80 mA.

Fig. 3 Micrographs showing the effect of current on the growth of HAp crystals (a, d) 5 mA, (b, e) 40 mA, (c) 80 mA. The area marked by a red circle indicates the hollow structure.

Fig. 4 SEM micrographs of HAp obtained in the hydrogel swelled in $CaCl_2$ (Tris-HCl, pH = 9.0) solution with simple ion diffusion method at 37 °C.

Fig. 5 SEM micrographs of HAp obtained in a hydrogel swelled in pure $CaCl_2$ solution using a simple ion diffusion method (a) the view of a whole sphere; (c) the view of a cross section. Panels b and d are the magnified pictures of panels a and c, respectively. The as-prepared hydrogel was swelled to 95 wt% water content. The solid domain was marked by a red circle.

Fig. 6 SEM micrographs of crystallization process of HAp crystals in the hydrogel at

different interval times (a) ~3 h (b) ~12 h (c) ~24 h (d) ~36 h.

Scheme 2 Schematic illustration of the formation mechanism of flower-like porous HAp spheres grown in the hydrogel (a - c). The PAAm chains provide a binding place for the Ca^{2+} ions (d). The black arrows and the red arrows indicate the diffusion direction of the ions, and the yellow arrows show the growth direction of HAp, respectively.

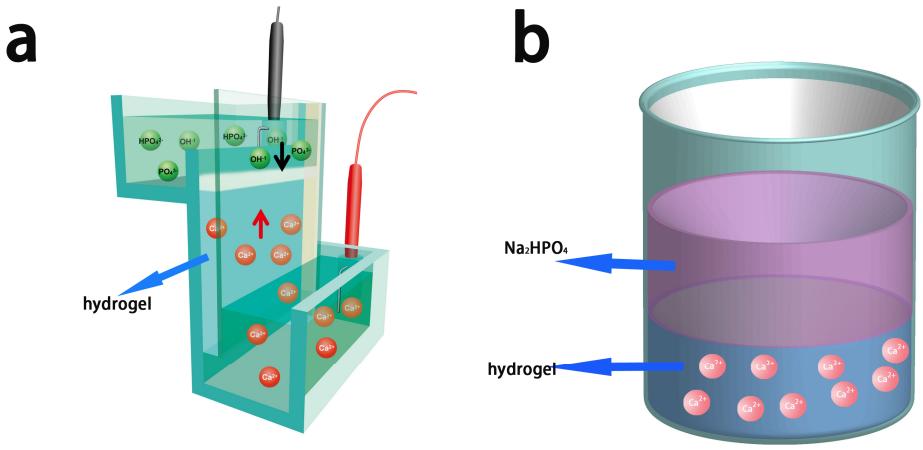

Scheme 1

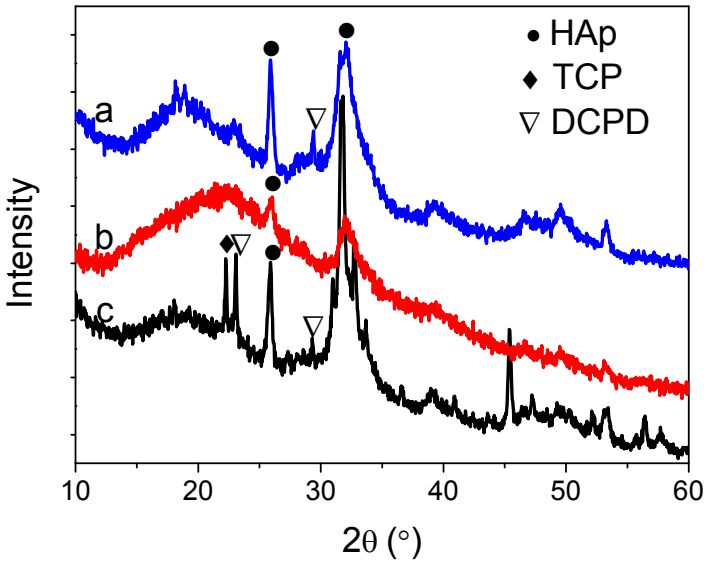

Fig. 1

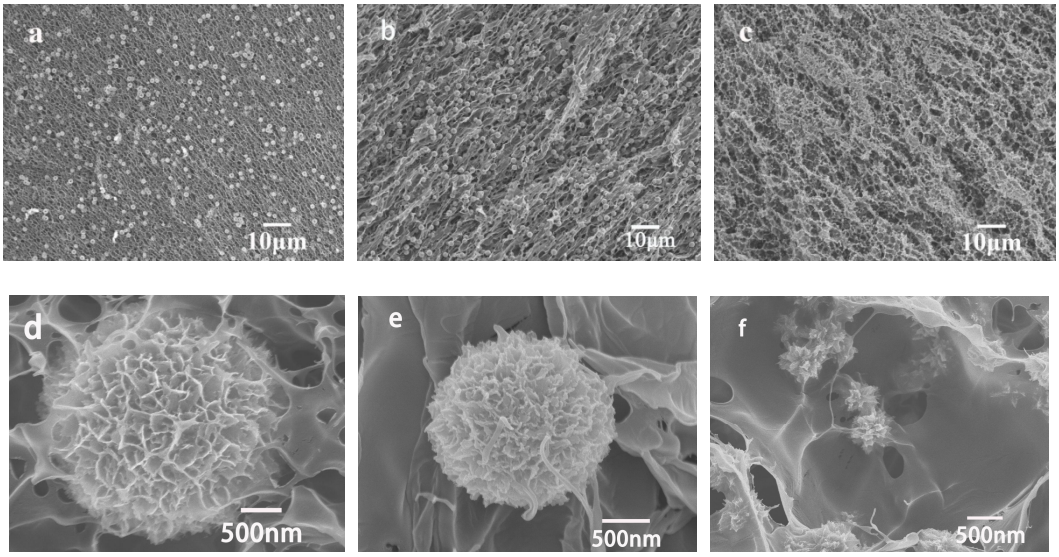

Fig. 2

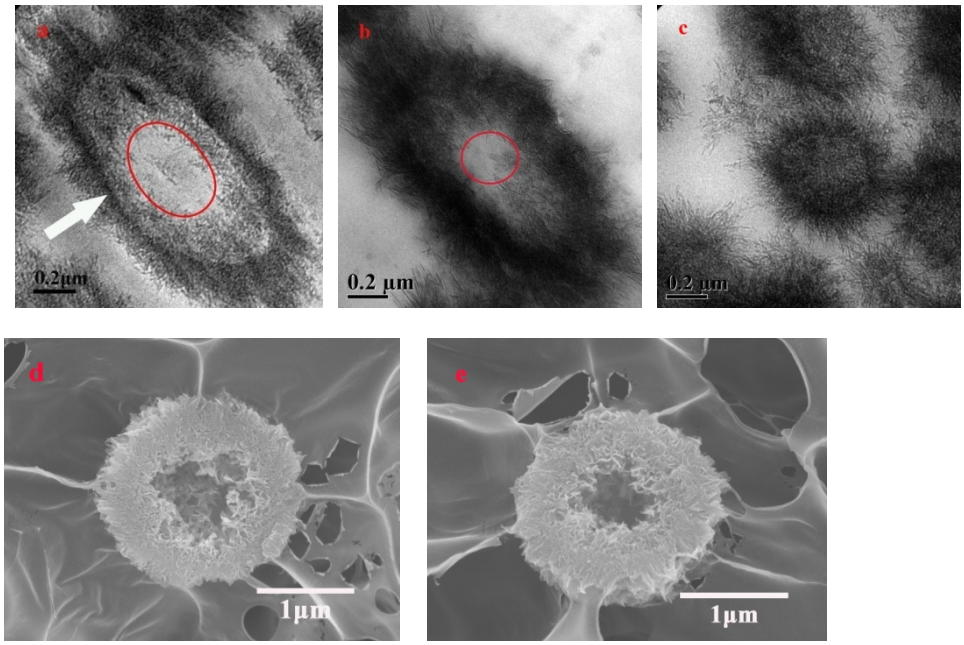

Fig. 3

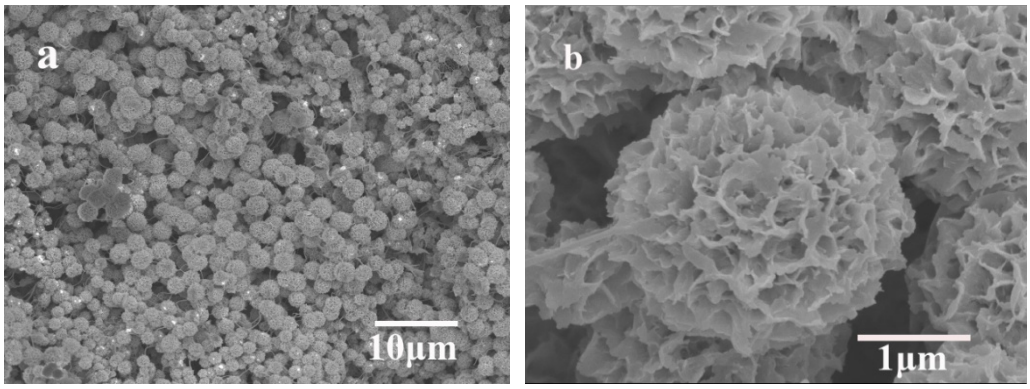

Fig. 4

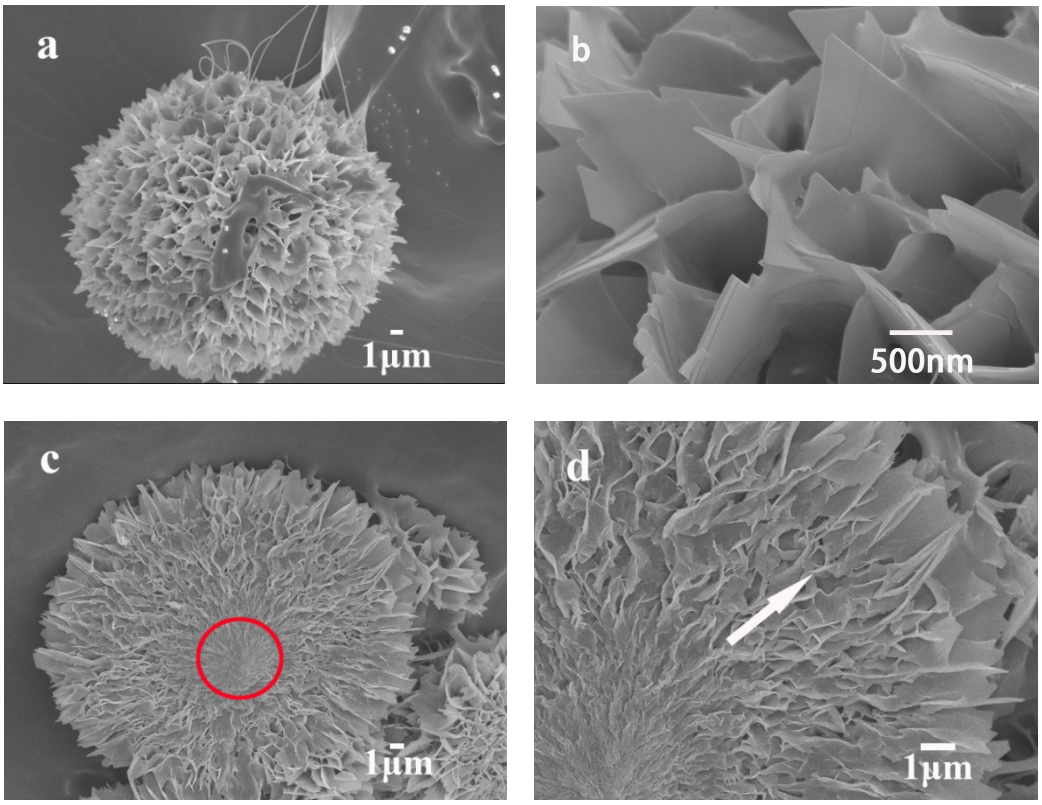

Fig. 5

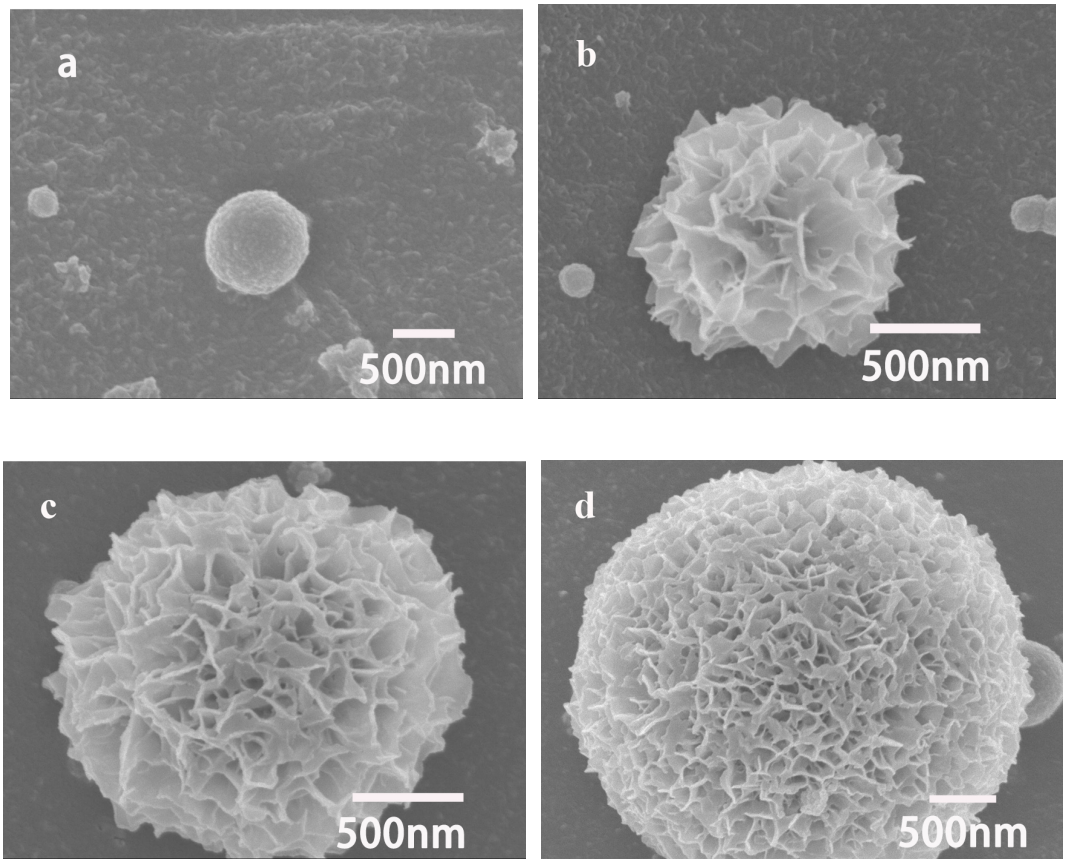

Fig. 6

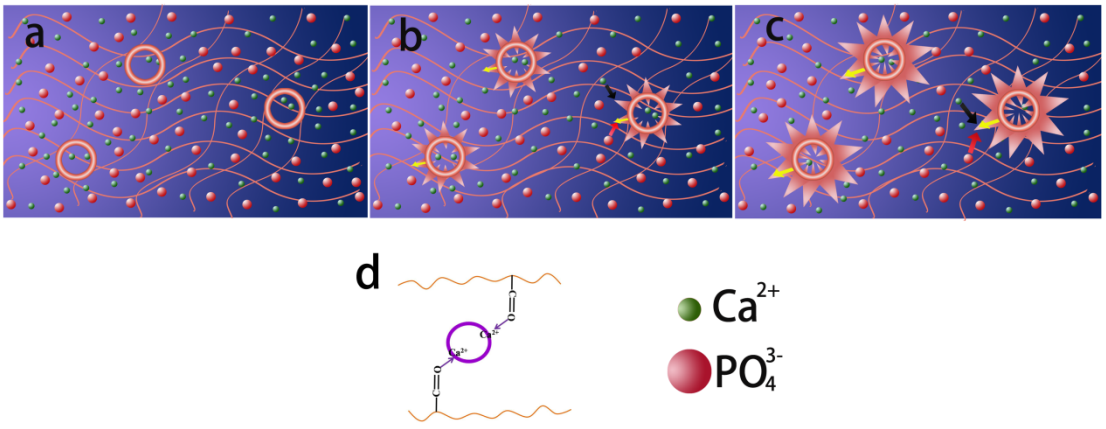

Scheme 2

A graphical and textual abstract

Flower-like porous hollow HAp spheres were obtained by diffusion of phosphate ions into PAAm hydrogels containing calcium ions by both electrophoresis approach and ion diffusion method. The flower-like porous hollow HAp spheres might be a combination result of hydrogel template and electrostatic interaction.